suggested that the ionized O_I center or this center in combination with a lattice defect is responsible for the growth of the Δ band.

The formation of the Δ band in the natural NaCl occurs only in localized areas. The portions of the crystal in which this colloid will appear can be predicted by close examination of the crystal after additive coloration. Faint dots of blue can be seen, and under a $100X$ microscope each blue dot has within it one or more bubbles. By reflected light the dot area shows Tyndall scattering. Since the natural crystals are grown from solution, it is reasonable to expect that the bubbles contain some water. During additive coloration the water reacts with the sodium, and now in these localized areas the initial conditions for promoting the growth of an absorbing type colloid are present. Optical absorption measurements in the immediate area of the bubble indicate the presence of a U band, and a trace of O_I band. The behavior, then, of the area immediately surrounding the bubbles in natural NaCl is identical with that of the bulk of the synthetic NaCl containing hydroxyl ion impurities.

Scattering type colloids which decorate grain boundaries form in all sodium chloride crystals which are slowly cooled from the additive coloring temper-

ature. It appears reasonable to conclude from the present work that the formation of an absorbing type colloid band in additively colored sodium chloride is due to the presence of impurities acting as nucleation centers. The formation of absorbing type colloid bands[9] observed in other alkali halides after additive coloration may be due to the presence of hydroxyl ions[6,10] in these melt grown crystals.

Since the natural crystal contains no hydroxyl ions, the areas in the crystal free of bubbles contain F centers after additive coloration. These F centers are present whether the crystal is slowly cooled or quenched from the additive coloring temperature; the only optical difference is that the slowly cooled crystal will also be decorated.

ACKNOWLEDGMENTS

[9] A. B. Scott, W. A. Smith, and M. A. Thompson, J. Phys. Chem. 57, 757 (1953).
[10] J. Rolfe, Phys. Rev. Letters 1, 56 (1956).

Crystal Potential and Energy Bands of Semiconductors. III. Self-Consistent Calculations for Silicon*

Leonard Kleinman† AND James C. Phillips‡
Department of Physics, University of California, Berkeley, California
(Received December 11, 1959)

An approximately self-consistent crystal potential is constructed for Si from a superposition of free-atom core and a sampling of crystal valence band charge densities. Valence-core exchange is calculated directly from core wave functions while valence-valence exchange is included using momentum-independent and momentum-dependent approximations taken from the results for a free-electron gas. The resulting crystal potential is surprisingly similar to one previously obtained by Woodruff from a superposition of free-atom charge densities. The calculated valence wave functions in the core region differ substantially from those of Woodruff because of the variational method used by him to calculate wave functions in that region. As a result the calculated energy gap is changed from Woodruff's value of 4 ev to about 1.5 ev, in substantially better agreement with the experimental value (1.1 ev). The various uncertainties in the calculation are listed; it is concluded that the relative position of levels near the band gap should be correct to within about 1 ev. Effective masses are also calculated and compared with experiment; the agreement is quite good.

I. INTRODUCTION

THIS is the third paper of a series[1,2] whose object is to present a careful study of the crystal potential seen by electrons in the covalently bonded semiconductors and to calculate the energy bands resulting

therefrom. The problem—rewarding in that experimental verification of the results is possible—is difficult on two counts. First there is the mathematical difficulty of obtaining good wave functions; this was solved for diamond by Herman[3] using the method of orthogonalized plane waves[4] (OPW) and by us in I using the repulsive potential method.[5]

[1] L. Kleinman and J. C. Phillips, Phys. Rev. 116, 880 (1959), hereafter called I.
[2] L. Kleinman and J. C. Phillips, Phys. Rev. 117, 460 (1960).

[3] F. Herman, Ph.D. thesis, Columbia University, 1953 (unpublished).
[4] C. Herring, Phys. Rev. 57, 1169 (1940).
[5] J. C. Phillips and L. Kleinman, Phys. Rev. 116, 287 (1959), hereafter called PK.

We regard the repulsive potential method as an approximation to the OPW method which has as its chief virtues its ease of calculation and the physical insight it lends to the problem. It is particularly well suited for demonstrating the error incurred by orthogonalization to incorrect core wave functions. In the next section we briefly review the repulsive potential method and discuss the best choice of core wave functions and the effect of incorrect functions on the repulsive potential.

Because of the second difficulty, obtaining the correct crystal and repulsive potential, none of the other valence semiconductors have previously been treated satisfactorily. In I we studied the valence electron contribution to the potential and showed that, at least for diamond, a simple superposition of atomic charge densities leads to a nearly self-consistent valence potential. This fact, together with the simplicity of the core, led to Herman's satisfactory results. There is no *a priori* reason to expect the same thing to be true for silicon. We therefore form our crystal charge density from an assembly of free atomic core charge densities arranged in the form of a diamond lattice plus a self-consistent crystal valence charge density. The self-consistent valence potential is discussed in Sec. IV where two choices for the exchange contribution are presented.

It is generally conceded that the most accurate crystal potential calculation for a polyvalent element beyond the second period was done by Heine[6] for aluminum. Because he could assume the valence wave functions to be single orthogonalized plane waves, he was able to aim for and probably achieve a relative accuracy of 0.02 ry in the energy levels. In doing silicon which lies next to aluminum in the periodic table, we shall be able to take advantage of some of Heine's work as the cores of the two atoms are to within a scaling factor almost identical. The core and repulsive potentials are calculated in Sec. III with an accuracy approaching Heine's. However, in going from aluminum to silicon, one goes from a case of nearly free valence electrons to the case of covalently bonded electrons. Because there exists no satisfactory treatment of exchange and correlation for this more general case, the relative accuracy of our final eigenvalues is limited to about 0.05 ry.

In the past few years two calculations of the energy bands of silicon have appeared. Woodruff[7] and Bassani,[8] who manufactured their crystal potential from a superposition of neutral atomic charge densities formed from analytic Slater[9,10] wave functions, would have obtained, had they carried their calculations to convergence, an indirect energy gap about 0.25 ry too large. Jenkins,[11] who manufactured his Hartree crystal potential from a superposition of singly charged silicon ion charge densities and used a cellular method of calculation, found

[6] V. Heine, Proc. Roy. Soc. (London) A240, 340 (1957).
[7] T. O. Woodruff, Phys. Rev. 103, 1159 (1956).
[8] F. Bassini, Phys. Rev. 108, 263 (1957).
[9] J. C. Slater, Phys. Rev. 36, 57 (1930).
[10] J. C. Slater, Phys. Rev. 42, 33 (1932).
[11] D. P. Jenkins, Proc. Phys. Soc. (London) A69, 548 (1956).

silicon to be a conductor. Because of the similarity in both method and results, we find it easy and instructive to compare our results with Woodruff's. The conclusions drawn from this comparison are that the crystal potential is insensitive to any reasonable approximation in either core or valence charge densities (a superposition of atomic valence wave functions is even closer to being self-consistent for silicon than for diamond) while the repulsive potential is very sensitive to approximations.

In Sec. V the energy bands are presented and because of our improvement over Woodruff's repulsive potential, agreement with the experimental energy gap and valence band width is obtained to within the uncertainties due to the valence-valence exchange.

In Sec. VI the effective masses of holes at the top of the valence band and electrons at the bottom of the conduction band are computed including the effect of the rapid oscillation of the wave functions in the atomic core region. Agreement with experiment is found to be quite good.

II. ORTHOGONALIZATION TO CORE LEVELS

We here give a short derivation of the repulsive potential method in order to obtain a simple means of displaying the physical significance of orthogonalization and the effects of small errors in the core wave functions upon orthogonalization.

Let us assume we know the crystal wave function ψ_α which transforms according to Γ_α, an irreducible representation of the cubic point group which has s or p atomic symmetry. Since ψ_α must be orthogonal to the core states of similar symmetry, $\psi_\alpha{}^n$, we can write

$$\psi_\alpha = \varphi_\alpha + \sum_n a_n{}^\alpha \psi_\alpha{}^n, \qquad (2.1)$$

$$a_n{}^\alpha = -(\varphi_\alpha, \psi_\alpha{}^n). \qquad (2.2)$$

We find the Schrödinger equation satisfied by φ_α, the "smooth" part of ψ_α by substituting (2.1) in the Schrödinger equation for ψ_α,

$$\mathcal{H}\psi_\alpha = E\psi_\alpha. \qquad (2.3)$$

Thus

$$\mathcal{H}\varphi_\alpha + \sum_n a_n{}^\alpha (E_n - E)\psi_\alpha{}^n = E\varphi_\alpha. \qquad (2.4)$$

If we now introduce

$$V_R = \frac{\sum_n a_n{}^\alpha (E_n - E)\psi_\alpha{}^n}{\varphi_\alpha}, \qquad (2.5)$$

we obtain

$$(\mathcal{H} + V_R)\varphi_\alpha = (-\nabla^2 + V + V_R)\varphi_\alpha = E\varphi_\alpha. \qquad (2.6)$$

If we now expand φ_α in a series of symmetrized plane waves transforming according to the irreducible representation Γ_α,

$$\varphi_\alpha = \sum_i b_i \sum_{\langle K_i \rangle} e^{i\langle K_i \cdot r \rangle} \qquad (2.7)$$

then applying the variational principle we obtain the

usual secular determinant

$$\det[V_T(K_j,K_i)+(k_i^2-E)\delta_{ij}]=0, \qquad (2.8)$$

where $V_T(K_j,K_i)$ represents the matrix element of $V+V_R$ between the ith and jth symmetrized combination of plane waves and consists of one or more Fourier transforms of $V+V_R$. Our secular equation (2.8) is like that obtained in the method of orthogonalized plane waves[4] but does not contain the complicated directionally dependent terms present there. Convergence of Eq. (2.8) is just as rapid as is obtained using OPW because Eq. (2.8) is the secular equation for the *smooth* part of the wave function. An examination of Eq. (2.5) shows the repulsive potential to be very nearly independent of angle because in the core region (where ψ_α^n is large) φ_α may for most irreducible representations, α, be approximated to very great accuracy by a radial function times the same spherical harmonic contained in ψ_α^n.

For those irreducible representations transforming with both s and p atomic symmetry (i.e., $\varphi_\alpha = a\varphi_\alpha^s + b\varphi_\alpha^p$) the repulsive potential may still be written in an angularly independent form:

$$V_R(r)=A V_R^s(r)+B V_R^p(r), \qquad (2.9)$$

where V_R^s and V_R^p are pure s and p repulsive potentials obtained using separately the s and p parts of φ_α in Eq. (2.5). In PK we showed how A and B may be obtained from a and b.

In the core region the radial part of φ_α may be approximated by a function of the form $r^l e^{-\beta r}$ where l is the azimuthal quantum number. The determination of β (as well as E) in a self-consistent manner is discussed in the next section. There it is also shown that this approximation causes only a small error which we almost completely eliminate by calculating the perturbation of the error on the energy levels. In return for this inconvenience we obtain not only a much easier method of calculation than OPW gives us, but also a means for displaying the physical significance of the orthogonalization terms.

Consider, for instance, the Fourier transforms of the effective potential listed in Table XI. One sees that all the Fourier transforms of the Coulomb potential but the (111) are very nearly cancelled by the repulsive potential seen by the s valence electrons while for p valence electrons the cancellation is not nearly so good. As we have pointed out in PK this is due to the fact that we have eliminated all the radial nodes in the wave functions but the p wave function contains an angular node that cannot be eliminated. If one adds the kinetic energy of the angular node [i.e., the centrifugal potential $l(l+1)/r^2$] to the p repulsive potential the sum is very nearly equal to the s repulsive potential. This explains the slow convergence of p wave functions in OPW calculations which has been a puzzle for some time. We might further note that it is the electrons' response to the lack of cancellation of V_{111} that causes the formation

of covalent bonds. In metals all the Fourier transforms (except V_{000}) are very nearly cancelled out by the repulsive potential; thus the electrons are nearly free.

Herring, in his original paper[4] discussed the errors which result from orthogonalizing to incorrect core wave functions. These errors are often of two types. The first results if the valence wave functions are orthogonalized to eigenfunctions of an incorrect Hamiltonian such as free atomic core wave functions rather than to core eigenfunctions of the crystal valence one electron Hamiltonian. Even if the core functions are eigenfunctions of the valence Hamiltonian, a second kind of error may occur if they are determined by a variational technique which leads to first-order errors in the wave functions. Woodruff[7] calculated the core eigenfunctions of silicon variationally while Heine[6] avoided the problem by calculation of the core eigenfunctions of aluminum numerically.

The repulsive potential method is particularly well suited for displaying these effects and a detailed discussion for silicon is given at the end of the next section.

III. CALCULATION OF CORE AND REPULSIVE POTENTIALS

There are no self-consistent calculations of the wave functions of the neutral silicon atom available in the literature; however, there exist both Hartree[12] and Hartree-Fock[13] calculations for the Si^{4+} ion. We wish to approximate the neutral silicon atom core with the Si^{4+} ion. As was pointed out by Heine,[6] neglecting the shielding of the valence electrons on the core causes only small variations in the core charge density. The Coulomb potential seen by the valence electrons is extremely insensitive to these small core variations. Furthermore, these small variations will be reduced if one approximates the neutral silicon atom by the Hartree Si^{4+} ion rather than the Hartree-Fock ion. For the effect of exchange is to increase the attractive potential seen by the core electrons and hence tends to cancel the shielding of the core electrons by the valence electrons. It can be seen that the neglect of exchange in the Hartree calculation does not overcompensate the neglect of valence electron shielding on the atomic cores since Table III shows that the Hartree ion eigenvalues calculated by McDougall[12] actually still lie below the experimental x-ray term values of the silicon atom.[14] We therefore took our core Coulomb potential from McDougall's Hartree calculation. It is listed in the second column of Table I as a function of r. The core-valence exchange potential is obtained from[15,6]

$$V_i^{\text{core-val ex}}(r_1)=\sum_\alpha \int \psi_\alpha(r_2)\frac{1}{r_{12}}\psi_i(r_2)dr_2\frac{\psi_\alpha(r_1)}{\psi_i(r_1)}, \qquad (3.1)$$

[12] J. McDougall, Proc. Roy. Soc. (London) A138, 550 (1932).
[13] W. Hartree, D. R. Hartree, and M. F. Manning, Phys. Rev. 60, 857 (1941).
[14] *American Institute of Physics Handbook* (McGraw-Hill Book Company, New York, 1957).
[15] J. C. Slater, Phys. Rev. 81, 385 (1951).

TABLE I. Contributions to $Z(r) = -rV(r)$ as seen by valence electrons in the spherical approximation. Column 2 lists the Coulomb contribution of the core. Columns 3 and 4 list the exchange contribution of the core with s and p valence electrons. Columns 5 and 6 list the exchange and Coulomb contributions of the valence electrons. Columns 7 and 8 are the sums of columns 2, 3, 5, 6, and 2, 4, 5, 6, respectively.

r	Z_{Coul}^{core}	$Z_{s\ exch}^{core-val}$	$Z_{p\ exch}^{core-val}$	$Z_{exch}^{val-val}$	Z_{Coul}^{val}	$Z(s)$	$Z(p)$
0.0050	13.767	0.039	0.036	0.006	−0.026	13.786	13.783
0.0247	12.883	0.217	0.192	0.028	−0.115	13.013	12.989
0.0451	12.080	0.352	0.285	0.051	−0.188	12.295	12.229
0.0672	11.335	0.458	0.337	0.076	−0.252	11.617	11.496
0.0907	10.668	0.547	0.359	0.103	−0.309	11.009	10.821
0.1165	10.042	0.669	0.368	0.132	−0.362	10.481	10.181
0.1572	9.204	0.429	0.380	0.179	−0.434	9.378	9.328
0.2019	8.413	0.340	0.412	0.229	−0.507	8.475	8.547
0.2725	7.349	0.512	0.498	0.309	−0.618	7.552	7.538
0.3679	6.225	0.634	0.623	0.418	−0.775	6.502	6.491
0.4966	5.213	0.743	0.765	0.564	−0.993	5.527	5.549
0.6703	4.502	1.132	1.083	0.761	−1.298	5.097	5.048
0.9048	4.140	−0.093	−0.215	1.027	−1.716	3.358	3.236
1.221	4.024	0.041	0.014	1.597	−2.248	3.414	3.387
1.649	4.0015	0.016	0.008	2.027	−2.832	3.212	3.204
2.014	4.0000	0.006	0.002	2.186	−3.200	2.992	2.988
2.460	4.0000	0.002	0.000	2.218	−3.503	2.717	2.715
3.004	4.0000	0.000	0.000	2.126	−3.728	2.398	2.398

where the summation is over the core states. The scaling of atomic wave functions has proved useful in extrapolating Hartree potentials[16] due to the insensitivity of valence electrons to small errors in core charge density; for the same reason it is possible to extrapolate Heine's aluminum core-valence exchange potential to silicon. By matching the nodes and maxima of the wave functions, one finds to a very good approximation in the core region

$$\psi_{Si}(r) = (1/0.95^{\frac{3}{2}})\psi_{Al}(r/0.95). \quad (3.2)$$

By substituting Eq. (3.2) into Eq. (3.1) one immediately finds

$$V_{Si}^{core-val\ ex}(r) = (1/0.95)V_{Al}^{core-val\ ex}(r/0.95), \quad (3.3a)$$

or

$$Z_{Si}^{core-val\ ex}(0.95r) = Z_{Al}^{core-val\ ex}(r), \quad (3.3b)$$

where $Z = -rV$.

The exchange potential (3.1) has been smoothed out over the region where it becomes infinite but this makes little error because of the node in $\psi_i(r_1)$. The valence wave functions used are the free atom wave functions which do not change appreciably in the core region on going to the crystal except for their normalization of which Eq. (3.1) is independent. Columns 3 and 4 of Table I list $Z^{core-val\ ex}(r)$ for s and p valence wave functions. Table II compares the Fourier transforms of $V^{core\ Coul}(r)$ and $V^{ocre-val\ ex}(r)$ with those of Woodruff. Because Woodruff used the Slater free-electron gas approximation[15]

$$V^{ex}(\mathbf{r}) = -6[(3/8\pi)\rho(\mathbf{r})]^{\frac{1}{3}} \quad (3.4)$$

for his total exchange potential, lumping both core and valence charge densities together, the separation of his exchange potential into core and valence terms is some-

what arbitrary. The separation was obtained by extrapolating his higher Fourier transforms, which result almost entirely from the core, down to the (111) transform. This procedure yields well-defined results because ρ_{val} is so extended that only the (111) transform is large (see Sec. IV).

We note that the difference between our s and p exchange potentials is small; hence small errors in $s-p$ character of the irreducible representations will lead only to small errors in the exchange potential. The similarity between Woodruff's $V^{core\ Coul}(K)$ and ours even though he used Slater wave functions for his core charge density confirms our earlier remarks about the insensitivity of the valence electrons to small changes in core charge density.

We now turn our attention to the calculation of the core eigenfunctions needed to calculate the repulsive potential. The contribution of the valence electrons to the crystal potential is calculated self-consistently in the next section; however, we need a spherical approximation to the valence electrons in the core region of an atom in the crystal in order to simplify the calculation of the core eigenfunctions.

It is assumed that the valence wave functions in the crystal can be approximated by a superposition of atomic-like wave functions on the crystal lattice sites whose smooth radial part has the form

$$\varphi_s = C_{3s}e^{-\alpha_s r}, \quad (3.5a)$$

$$\varphi_p = C_{3p}re^{-\alpha_p r}. \quad (3.5b)$$

α_s and α_p were chosen to give approximate agreement with ρ_{111} obtained self consistently. These smooth wave functions must be orthogonalized to the core eigenfunctions of the valence Hamiltonian which for this purpose we approximate by the analytic $1s$, $2s$, and $2p$ Slater[9,10] wave functions, obtaining for the radial part of

[16] D. R. Hartree, Proc. Cambridge Phil. Soc. 51, 684 (1955).

TABLE II. Comparison of Fourier coefficients of core contribution to potential with those of Woodruff. Column 2 lists Woodruff's core Coulomb term. Column 3 lists our core Coulomb term. Column 4 lists the exchange potential due to the core seen by Woodruff's valence electrons. Columns 5 and 6 list the exchange potential due to the core seen by our s and p valence electrons. Column 7 is the sum of columns 2 and 4. Column 8 is the sum of the average of columns 5 and 6 with column 3. The coefficients have not been multiplied by the form factor $\cos(\pi/4)(K_1+K_2+K_3)$.

$\left(\dfrac{a}{-K}\right)^2$	$V_W{}^{\text{core Coul}}(K)$	$V^{\text{core Coul}}(K)$	$V_W{}^{\text{core-val ex}}(K)$	$V_s{}^{\text{core-val ex}}(K)$	$V_p{}^{\text{core-val ex}}(K)$	$V_W{}^{\text{core}}(K)$	$V^{\text{core}}(K)$
3	−0.737	−0.754	−0.050	−0.041	−0.037	−0.787	−0.793
8	−0.328	−0.334	−0.044	−0.035	−0.033	−0.371	−0.368
11	−0.258	−0.263	−0.042	−0.032	−0.031	−0.300	−0.294
16	−0.191	−0.201	−0.039	−0.028	−0.027	−0.230	−0.229
27	−0.131	−0.141	−0.029	−0.023	−0.022	−0.160	−0.163
40	−0.103	−0.108	−0.019	−0.016	−0.017	−0.122	−0.124
64	−0.075	−0.077	−0.008	−0.009	−0.009	−0.083	−0.086

the wave functions

$$\psi_{3s}=0.9104[e^{-0.566r}-26.79re^{-4.295r}+6.625e^{-13.7r}], \quad (3.6a)$$

$$\psi_{3p}=1.636r[e^{-1.13r}-11.39e^{-4.925r}]. \quad (3.6b)$$

We choose our atom to have $(17/8)$ p electrons and $(15/8)$ s electrons as this is approximately the number of each in the valence band averaged over the Brillouin Zone (see Table V). The potential due to these valence electrons is computed from Poisson's equation

$$\nabla^2 V=-8\pi\rho, \quad (3.7)$$

and Slater's[15] free electron exchange approximation [Eq. (3.4)].

Due to the nonlocal nature of the exchange potential the rapid oscillations of the valence charge density in the core will not be seen by the valence electrons and following Heine[6] we have therefore averaged the charge density over the core before inserting it in Eq. (3.4).

It should be mentioned that the spherical approximation neglects the overlap of charge density from other crystal sites. Hence there is an unavoidable error in the Hamiltonian for which we are calculating the eigenfunctions. In the core region this overlapping charge density should be small and approximately constant. Neglecting this overlap is therefore equivalent to making E_n slightly too negative. On the other hand, we found after calculating ρ_{111} self-consistently that α_s and α_p and hence the shielding due to the valence electrons were too large. As these errors are in opposite directions and each causes an error in the repulsive potential of less than 0.01 ry, no attempt was made to correct them. Columns 5 and 6 of Table I list $Z^{\text{val-val ex}}(r)$ and $Z^{\text{val Coul}}(r)$. We

TABLE III. Eigenvalues of $1s$, $2s$, and $2p$ core functions in ry determined in four different ways.

	$1s$	$2s$	$2p$
Hartree[a]	−141.20	−14.135	−11.230
Woodruff's variational	−134.597	−11.1237	−8.17697
Present calculation	−131.4208	−12.00415	−8.72145
Atomic x-ray term values[b]	−135.4	−11.0	−7.3

[a] See reference 12.
[b] See reference 14.

repeat that these spherical valence potentials are used only to compute the lower eigenvalues and eigenfunctions of the valence Hamiltonian. Columns 7 and 8 of Table I list the total spherical potential for s and p electrons, respectively.

To facilitate the numerical integration of the radial part of the Schrödinger equation the following substitutions are made[17]:

$$\rho=\ln r, \quad (3.8a)$$

$$P'=Pr^{-\frac{1}{2}}=\psi r^{\frac{1}{2}}. \quad (3.8b)$$

This gives

$$(d^2P'/d\rho^2)+[Ee^{2\rho}+2Ze^\rho-(l+\tfrac{1}{2})^2]P'=0 \quad (3.9)$$

in atomic units (E in ry, r in Bohr radii) which was integrated with the boundary condition $(d\psi/dr)_{r_s}=0$, where $Z=-rV(r)$ and r_s is the radius of the equivalent volume sphere ($r_s=3.18$). Table III lists the eigenvalues for the $1s$, $2s$, and $2p$ eigenfunctions and compares them with those of Woodruff and the Hartree core wave functions. We note that Woodruff's variational eigenvalues lie above ours with the exception of the $1s$. This is because he did not average the charge density over the core before computing the exchange potential and so his exchange potential is much too great in the $1s$ region of the core.

The repulsive potentials are obtained from Eqs. (2.5) and (2.2) by inserting these calculated $1s$, $2s$, and $2p$ eigenfunctions and eigenvalues into Eq. (2.5) and approximating φ_α by φ_s and φ_p of Eq. (3.5a, b). Table IV gives the $1s$ and $2s$ repulsive potential as a function of r for $\Gamma_{2'}$ and the $2p$ repulsive potential for Γ_{15} and the total spherical potential (including repulsive) for $\Gamma_{2'}$ and Γ_{15}. Figure 1 is a graph of the total spherical potential for $\Gamma_{2'}$.

The percentage of s and p repulsive potential to be used in each irreducible representation was determined by a preliminary expansion of its symmetrized combinations of plane waves into products of spherical harmonics and radial functions. These were then integrated over the core eigenfunctions yielding essentially weighted sums of the orthogonalization contribution to

[17] D. R. Hartree, Phys. Rev. 46, 738 (1934).

TABLE IV. Charge $Z(r) = -rV(r)$ due to repulsive (orthogonalization) potential in spherical approximation. Columns 2 and 3 list the $1s$ and $2s$ repulsive contributions to $\Gamma_{2'}$ which are totaled in column 4. Column 5 is the repulsive charge seen by Γ_{15} levels. Columns 6 and 7 list the total effective charge seen by $\Gamma_{2'}$ and Γ_{15} levels which is obtained by adding the repulsive charge to $Z(s)$ for $\Gamma_{2'}$ and to $Z(p)$ for Γ_{15}. $Z(s)$ and $Z(p)$ are listed in Table I.

r	$Z_R^{1s}(\Gamma_{2'})$	$Z_R^{2s}(\Gamma_{2'})$	$Z_R(\Gamma_{2'})$	$Z_R(\Gamma_{15})$	$Z^{\text{eff}}(\Gamma_{2'})$	$Z^{\text{eff}}(\Gamma_{15})$
0.0050	−5.088	0.692	−4.396	−0.661	9.390	13.122
0.0247	−17.612	2.379	−15.323	−2.847	−2.310	10.142
0.0451	−24.811	3.225	−21.586	−4.662	−9.291	7.567
0.0672	−28.080	3.399	−24.681	−6.213	−13.064	5.283
0.0907	−28.347	2.992	−25.355	−7.469	−14.346	3.352
0.1165	−26.537	2.104	−24.433	−8.481	−13.952	1.700
0.1572	−21.776	−0.223	−21.553	−9.495	−12.175	−0.167
0.2019	−16.264	−2.006	−18.270	−10.022	−9.797	−1.475
0.2725	−9.662	−4.937	−14.599	−10.077	−7.047	−2.539
0.3679	−4.170	−8.012	−12.182	−9.375	−5.680	−2.884
0.4966	−1.275	−9.580	−10.855	−7.954	−5.328	−2.405
0.6703	−0.259	−9.117	−9.376	−6.023	−4.279	−0.975
0.9048	−0.070	−6.618	−6.688	−3.849	−3.330	−0.613
1.221	−0.017	−3.739	−3.756	−2.143	−0.342	1.244
1.649	−0.005	−1.546	−1.551	−1.004	1.661	2.200
2.014	−0.001	−0.683	−0.684	−0.528	2.308	2.460
2.460	0	−0.250	−0.250	−0.256	2.467	2.460
3.004	0	−0.127	−0.127	−0.117	2.271	2.281

the diagonal matrix elements in the OPW method [see Eqs. (3.10) and (3.11)]. The percentage of s and p repulsive potential was then taken equal to be the percentage of the s and p contributions to these sums. Although in principle the percentage of s and p repulsive potential can be calculated exactly, it is extremely difficult in practice and of not much advantage as our spherical approximation for φ_α has already introduced some error into the repulsive potential. In Table V is listed the percentage of s and p repulsive potential used in each irreducible representation. We estimate it to be accurate to within about 3%.

The error introduced in the repulsive potential is corrected as follows. The contribution of the orthogonalization terms to the matrix element in the OPW method is given by

$$\sum_{nl} (E - E_{nl}) A_{nl}^*(k_i) A_{nl}(k_j) \sum_{k_j - k_i} P_l(\cos\theta_{ij})$$

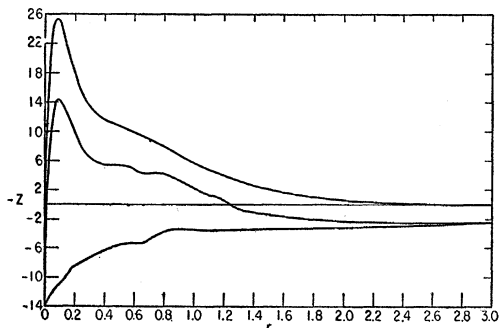$$\times \sum_{\nu}^{\text{cell}} e^{i(k_j - k_i) \cdot R_\nu}, \quad (3.10)$$

where

FIG. 1. Graph of $-Z(r) = rV(r)$. The lower curve is the Coulomb and exchange charge. The upper curve is the repulsive or orthogonalization charge for the $\Gamma_{2'}$ level. The middle curve is their sum, the total effective charge for the $\Gamma_{2'}$ level.

$$A_{nl}(k) = \frac{1}{\Omega_0^{\frac{1}{2}}} \int_\infty \psi_{nl}(\mathbf{r}) e^{i\mathbf{k} \cdot \mathbf{r}} d\tau$$

$$= \left[\frac{4\pi(2l+1)}{\Omega_0}\right]^{\frac{1}{2}} i^l \int_0^\infty r^2 \psi_{nl}(r) j_l(kr) dr, \quad (3.11)$$

where $P_l(\cos\theta_{ij})$ is the lth Legendre polynomial of the angle between $\mathbf{k}_i$ and $\mathbf{k}_j$, the sum over n, l is over core functions, the sum over $\mathbf{k}_j - \mathbf{k}_i$ is over all $\mathbf{k}_j - \mathbf{k}_i$ appearing in the product of the ith and jth symmetrized combination of plane waves, $\mathbf{R}_\nu$ is a vector to each atom in the unit cell, Ω_0 is the normalization constant for the plane waves, and $j_l(kr)$ is the lth spherical Bessel function. The difference between the contribution obtained from the repulsive potential, $\sum_{\mathbf{k}_i - \mathbf{k}_j} V_R(\mathbf{k}_i - \mathbf{k}_j)$, and by OPW is listed in Table VI for certain matrix elements and all solutions of all irreducible representations of interest.

We shift all diagonal elements of a matrix so as to make the error in the diagonal element of interest zero

TABLE V. Percentage of s and p repulsive potential used in computing various crystal eigenstates.

	s	p
$\Gamma_{12'}$	0	0
Γ_1	1.00	0
$\Gamma_{25'}$	0	1.00
Γ_{15}	0	1.00
$\Gamma_{2'}$	1.00	0
$\Gamma_1^{(2)}$	1.00	0
$L_1^{(1)}$	0.95	0.05
L_2^1	0.95	0.05
$L_{3'}$	0	1.00
L_3	0	1.00
$L_1^{(2)}$	0.95	0.05
$X_1^{(1)}$	0.95	0.05
X_4	0	1.00
$X_1^{(2)}$	0.95	0.05

[i.e., the (11) element if we want the lowest solution or the (22) element if we want the next lowest]. The correction which must be made when the matrix is now diagonalized is given by first-order perturbation theory as

$$\delta E_k = \sum_{ij} \delta V_{ij} a_i a_j, \quad (3.12)$$

where a_j is the amplitude of the jth symmetrized combination of plane waves appearing in the kth eigenfunction transforming according to some particular irreducible representation and δV_{ij} is the error in the (ij)th matrix element (δV_{kk} is now zero). δE_k was calculated cutting the sum over i and j off at $k-1 \leq i$, $j \leq k+1$ and is listed in the last column of Table VI. We can make several interesting observations about these corrections. We note that the largest correction computed is less than 0.015 ry and estimate the largest error made by cutting off the sum (3.12) to be of order 0.005 ry. The signs of the corrections for X_1, $L_{2'}$ and L_1 indicate that we chose $X_1^{(1)}$, $L_1^{(1)}$ and $L_{2'}$ to have too much p

character and $X_1^{(2)}$ and $L_1^{(2)}$ to have too little p character. We note that in general the errors in the matrix elements of p-like irreducible representations are larger than those in s-like. There are two reasons for this. Firstly, even at the center of the Brillouin Zone the eigenfunctions of these irreducible representations are not pure s or p but have small amounts of higher angular symmetry mixed in; p eigenfunctions have small amounts of d and higher symmetry mixed in, while s eigenfunctions tend to have smaller amounts of g and higher symmetry mixed in. Secondly, the p repulsive potential is much more sensitive to errors in the approximation of φ_α by φ_s and φ_p. From Eqs. (2.5) and (2.2) we see that V_R depends only on the shape of φ_α and not its normalization. φ_s is fairly flat in the core region and hence not sensitive to small errors in the exponential by which it is approximated, while φ_p is an increasing function in the core region and hence sensitive to errors in its shape.

The repulsive potential is most sensitive to the core orbitals $\psi_\alpha{}^n$. To illustrate the way in which different choices of $\psi_\alpha{}^n$ affect the repulsive potential, Table VII lists Fourier transforms of repulsive potentials obtained from three different $2p$ wave functions: (1) our $2p$ wave function which is obtained by direct integration of the Schrödinger equation using the valence one electron Hamiltonian; (2) the Hartree $2p$ wave function which is also obtained by direct integration but which uses the core Hamiltonian; (3) Woodruff's $2p$ wave function which is an eigenfunction of a valence Hamiltonian very nearly the same as ours but which is subject to first-order errors because it was obtained variationally. The Hartree core functions are seen to yield too large and Woodruff's too small a repulsive potential.

The main reason for the Hartree wave functions yielding too large a repulsive potential is that their eigenvalues, E_n, are much lower than those of the core eigenfunctions of the valence Hamiltonian. The core electrons see a larger nuclear charge than the valence electrons due to the valence electrons being screened by all the core electrons while each core electron is screened only by the *other* core electrons. Thus the core wave functions are pulled in tighter and have lower energy than the eigenfunctions of the valence Hamiltonian. On

TABLE VI. Errors in ry in various matrix elements incurred by using the repulsive potential rather than OPW. The last column lists the error in the various eigenvalues due to these errors after a constant has been added to the diagonal matrix elements.

	(11)	(22)	(33)	(21)	(32)	δE
$\Gamma_1^{(1)}$	0.04866	0.02972		-0.00177		0.00019
$\Gamma_{25'}^{(1)}$	0.08728	0.06111		0.02086		-0.01097
$\Gamma_{15}^{(1)}$	0.09068	0.05081		0.00727		-0.00085
$\Gamma_{2'}^{(1)}$	0.03346	0.04466		0.01356		-0.00508
$L_1^{(1)}$	0.07254	0.00238		-0.00744		0.00895
$L_{2'}^{(1)}$	0.04512	0.03587		0.00744		0.00255
$L_{3'}^{(1)}$	0.07886	0.15849		-0.01426		-0.00583
$L_3^{(1)}$	0.08669	0.08732		-0.01481		-0.00826
$X_1^{(1)}$	0.07275	0.04396		-0.01358		0.01355
$X_4^{(1)}$	0.05932	0.09902		0.01959		-0.01422
$X_1^{(2)}$	0.07693	0.04910	0.19005	-0.01304	-0.02018	-0.00749
$L_1^{(2)}$	0.08757	0.00736	0.35307	-0.00723	0.04074	-0.00755
$\Gamma_1^{(2)}$	0.05485	0.03345	0.36266	-0.00119	0.007275	-0.00110

the other hand, Woodruff's core eigenfunctions yield too weak a repulsive potential because the tail of a wave function does not affect the energy very strongly; it therefore is poorly determined by a variational calculation. However, the tail of the core function makes a large contribution to the repulsive $2p$ potential because the product of the core and smooth valence p functions is large in the tail of the core function. The three $2p$ functions are compared in Fig. 2. The differences are seen to be small, emphasizing the importance of a very accurate calculation of the core eigenfunctions of the valence Hamiltonian.

Table VII also lists the s repulsive potential Fourier transforms calculated by Woodruff and by us. The $2s$ potentials are seen to be much more nearly alike than are the $2p$. This is because although the $2s$ repulsive potential is equally as sensitive to errors in eigenvalue as is the $2p$, it is less sensitive to the shape of the eigenfunctions. The relatively large error in Woodruff's $1s$ repulsive potential is due to his use of the Slater wave function rather than a variational wave function for ψ_{1s}.

That the p repulsive potential is more sensitive to any source of error in the shape of the core wave functions than is the s can be shown analytically, by considering the factor $a_n{}^\alpha$ appearing in the repulsive potential [Eqs. (2.5) and (2.2)]. In the core region to a first approximation the smooth part of the $3s$ wave function is a constant and the smooth part of the $3p$ wave function

TABLE VII. Comparison of Fourier coefficients of repulsive potential. Columns 2, 3, and 4 list the repulsive potential for the eigenstate Γ_{15} as computed from the $2p$ eigenfunction and eigenvalue of Woodruff, of a Hartree core calculation, and of us. Columns 5 and 6 list the $2s$ and $1s$ contribution to Woodruff's $\Gamma_{2'}$ repulsive potential listed in column 7. Columns 8 and 9 list the $2s$ and $1s$ contribution to our $\Gamma_{2'}$ repulsive potential listed in column 10. The coefficients have not been multiplied by the form factor $\cos(\pi/4)(K_1+K_2+K_3)$.

| $\left(\dfrac{a}{2\pi}K\right)^2$	$V_R{}^W(\Gamma_{15})$	$V_R{}^H(\Gamma_{15})$	$V_R(\Gamma_{15})$	$V_R{}^W(2s)$	$V_R{}^W(1s)$	$V_R{}^W(\Gamma_{2'})$	$V_R(2s)$	$V_R(1s)$	$V_R(\Gamma_{2'})$
3	0.2974	0.495	0.3909	0.5153	0.0766	0.5919	0.5178	0.1003	0.6181
8	0.2240	0.350	0.2653	0.3380	0.0750	0.4130	0.3322	0.0970	0.4292
11	0.1934	0.294	0.2213	0.2671	0.0740	0.3411	0.2623	0.0952	0.3575
16	0.1558	0.232	0.1734	0.1847	0.0725	0.2572	0.1834	0.0924	0.2758
27	0.1061	0.155	0.1151	0.0879	0.0693	0.1572	0.0899	0.0868	0.1768
40	0.0748	0.108	0.0787	0.0386	0.0657	0.1043	0.0398	0.0812	0.1209
64	0.0463	0.067	0.0476	0.0063	0.0598	0.0661	0.0061	0.0724	0.0784
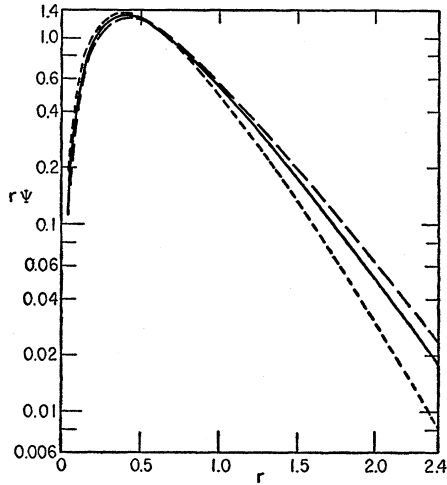
FIG. 2. Logarithmic graph of the $2p$ wave function determined as Hartree solution to core Hamiltonian (solid line), eigenfunction of valence Hamiltonian (long-dashed line), variational eigenfunction of Woodruff's valence Hamiltonian (short-dashed line).

increases as r; hence

$$a_{2s} \sim \int \psi_{2s} d\tau, \qquad (3.13a)$$

$$a_{2p} \sim \int \psi_{2p} r d\tau. \qquad (3.13b)$$

But

$$\delta \int \psi^2 d\tau = \int \psi \delta \psi d\tau = 0 \qquad (3.14)$$

indicates that $\delta\psi$, the error in ψ, tends to be positive about as much as it is negative. Therefore δa_{2s} is small but δa_{2p} (which is weighted by an extra factor of r) may be quite large if (as is usually the case) the sign of $\delta\psi_{2p}$ changes only once (see Fig. 2). Hence Woodruff's variational determination of the core functions was satisfactory for the s repulsive potential but not the p.

The qualitative argument we have just given in terms of the repulsive potential can also be given an OPW interpretation. With the definitions

$$j_0(X) = \sin X / X \quad \text{and} \quad j_1(X) = \sin X / X^2 - \cos X / X,$$

we see from Eq. (3.11) that the s orthogonalization terms of the OPW method consist of a single integral involving the core functions while the p terms consist of

TABLE VIII. Comparison of OPW orthogonalization coefficients. A_{2p} is equal to the difference between $A_{2p}{}^{\sin}$ and $A_{2p}{}^{\cos}$ and therefore is much more sensitive to errors then A_{2s} which consists of a single integral.

	$A_{2p}{}^{\sin}$	$A_{2p}{}^{\cos}$	$A_{2p}{}^{[(2/\pi a)(111)]}$	$A_{2s}{}^{[(2/\pi a)(111)]}$
Woodruff	0.34712	0.27665	0.07047	0.1388
Present calculation	0.35795	0.26647	0.09148	0.1377

the *difference* between two such integrals and hence are susceptible to much larger errors. This is demonstrated for $A_n[(2\pi/a)(111)]$ in Table VIII, using both Woodruff's core wave functions and ours.

IV. SELF-CONSISTENT VALENCE POTENTIAL

The nonzero Fourier transforms of the Coulomb potential due to the smooth part of the valence charge density are given by

$$V_{\mathbf{K}} = \frac{64\pi}{K^2 a^3 \tau_k} \int_{\text{B.z.}} \rho_{\mathbf{K}}(\mathbf{k}) d\tau_k, \qquad (4.1)$$

where $\rho_{\mathbf{K}}(\mathbf{k})$ is the amplitude of the $\mathbf{K}$th Fourier component of the smooth part of the charge density of all electrons with wave vector $\mathbf{k}$ in the first Brillouin zone and τ_k is the volume of the Brillouin zone. We have pointed out in I that the integration over the Brillouin zone may be replaced by a summation of $\rho_{\mathbf{K}}(\mathbf{k})$ over points $\mathbf{k}$ determined as follows. Reciprocal space is

TABLE IX. The contribution of charge densities representing different sub-zones in the valence band to the Fourier coefficients of the crystal potential using both exchange potentials described in the text. The last line lists the total $= \{\Gamma\} + \{X\} + \{L\}$. Each of the latter represents the contribution of each term multiplied by the degeneracy and weighting factors listed in columns 2 and 3.

Term	Degeneracy	Weight	V_{111}	V_{220}	$V_{111}{}^{k\ \text{dep}}$	$V_{220}{}^{k\ \text{dep}}$
Γ_1	1		0.004514	0.0000785	0.005410	-0.0001799
$\Gamma_{25'}$	3		0.007852	-0.0000770	0.007559	-0.0001236
$\{\Gamma\}$		1	0.02807	-0.000152	0.02809	-0.000551
X_1	2		0.005975	0.0000469	0.006634	0.0001218
X_4	2		0.005132	-0.0005175	0.004638	-0.0005305
$\{X\}$		3	0.06664	-0.002824	0.06763	-0.002452
L_1	1		0.002354	-0.0001169	0.003756	-0.0000094
$L_{2'}$	1		0.005992	0.0002402	0.006556	0.0003374
$L_{3'}$	2		0.005902	-0.0004657	0.005860	-0.0004821
$\{L\}$		4	0.08060	-0.003233	0.08813	-0.002544
8Γ			0.22456	-0.00122	0.22472	-0.00441
Total			0.17531	-0.00621	0.18385	-0.00555

divided into similar volumes resembling the first Brillouin zone. The first division used the B.z. about each reciprocal lattice point; the second division refines the first by introducing new subreciprocal lattice points midway between the lattice points of the first division. New subzones are now drawn about each of the points of the new lattice (which includes all the points of the previous lattice). The subzones are similar to the original zone, but have 2^{-3} the volume. This mesh process can be used to obtain an arbitrarily fine covering of reciprocal space and $\rho_{\mathbf{K}}(\mathbf{k})$ is summed over the subreciprocal lattice points. Thus the first approximation to $(1/\tau)\int \rho_{\mathbf{K}}(\mathbf{k}) d\tau_k$ is

$$\{\Gamma_1\} + 3\{\Gamma_{25'}\}, \qquad (4.2)$$

and the second approximation is

$$\frac{1}{8}[\{\Gamma_1\} + 3\{\Gamma_{25'}\} + \sum_1^4 (\{L_1\} + \{L_{2'}\} + 2\{L_{3'}\})$$

$$+ \sum_1^3 (2\{X_1\} + 2\{X_4\})], \qquad (4.3)$$

TABLE X. Comparison of Fourier coefficients of valence contribution to potential with those of Woodruff. Columns 2 and 3 list Woodruff's valence Coulomb and valence exchange contributions. Because of the form of his exchange potential it is not possible to separate out the small valence contributions to the higher Fourier coefficients. Columns 4 and 5 list our self-consistent valence Coulomb Fourier coefficients for the momentum independent and dependent valence-valence exchange potentials, the Fourier coefficients of which are listed in columns 6 and 7. The coefficients have not been multiplied by the form factor $\cos(\pi/4)(K_1+K_2+K_3)$.

$\left(\dfrac{a}{2\pi}K\right)^2$	V_W val Coul	V_W val-val ex	$V_{k\text{-indep}}$ val Coul	$V_{k\text{-dep}}$ val Coul	$V_{k\text{-indep}}$ val-val ex	$V_{k\text{-dep}}$ val-val ex
3	0.1468	−0.0778	0.1451	0.1518	−0.0669	−0.0467[a] −0.0933[b]
8	−0.0074	?	−0.021		0.013	
11	−0.0078	?	−0.010		0.007	
16	−0.0038	?	−0.005		0.004	
27	−0.0029	?	−0.002		0.002	
40	0.0003	?				
64	0.0002	?				

[a] For all other states.
[b] For states $L_1^{(1)}$, $L_{2'}^{(1)}$, $\Gamma_1^{(1)}$, $X_1^{(1)}$.

where { } denotes $\psi^*\psi$ for a nondegenerate level and the average of $\psi^*\psi$ for degenerate levels and the summations are over the four (111) directions and three (100) directions. Higher approximations require wave functions for general points in k space making the calculation feasible only with the largest digital computers. Inspection of Table IX will indicate that V_{111} is probably given quite well by the second approximation. Columns 4 and 6 list the self-consistent (in the second approximation) smooth valence Coulomb V_{111} for two different valence exchange potentials. In the extended zone scheme the first approximation consists of the charge density at the bottom of the zone plus thrice the charge density at the top of the zone—a very poor sampling indeed. In the second approximation we sample at 28 additional points spaced throughout the zone. Hence since the charge density varies slowly throughout the zone,[18] one expects the change in going from the first to the second approximation to be much larger than any change in going to higher approximations. Table IX shows this first change to be less than 0.05 ry; hence we estimate the error in the second approximation to be 0.01 or at most 0.02 ry. V_{220} is seen from Table IX to be 0.006 ry and all higher Fourier transforms will be even smaller; hence the error in the (220) and higher Fourier transforms is of order 0.003 ry.

The large negative value of V_{111} is due to valence electrons from all over the Brillouin zone responding to the large (111) component of potential [due to the atomic cores lying along (111) directions]; while the contributions to V_{220} from different points in the B.z. are seen to add with random sign.

The total valence Coulomb potential is determined by writing the wave functions in the form of Eq. (3.5a, b) with the parameters chosen so V_{111} computed from the leading terms agrees with V_{111} in Table IX. Then the renormalization of the smooth part of the wave function

(due to the addition of the nodes) and the contribution of the nodes to the potential can be calculated straightforwardly. The fourth and fifth columns in Table X list Fourier transforms of the total valence Coulomb potential for the two different exchange potentials discussed below. A remarkable similarity is seen to exist in Table X between the self-consistent valence Coulomb potential and the valence Coulomb potential constructed by Woodruff from a superposition of spherical free-atom Slater wave functions for all Fourier transforms except the zeroth.

The zeroth Fourier transform of the Coulomb potential is given for a spherical charge density, $\rho(r)$, by[19]

$$\lim_{K\to 0}\frac{16\pi^2}{3\Omega_0}\int \rho(r)r^4 dr. \qquad (4.4)$$

One would not expect a superposition of spherical charge densities to yield V_{000} correctly because it weights $\rho(r)$ strongly for large values of r—just where the spherical approximation is worst. We therefore estimated the total Coulomb and exchange contribution to V_{000} as follows. The energy required to remove the four valence electrons from a free atom of silicon is 7.58 ry; the cohesive energy of silicon is 0.27 ry per atom; the average valence electron energy per silicon atom in the crystal is therefore -7.85 ry. The only effect of V_{000} on the relative positions of the energy bands is through its effect on the absolute position of the levels which enter the repulsive potential through the factor $(E-E_n)$. We therefore determine the V_{000} which will lead to absolute values of the energy bands which when averaged over the Brillouin zone (in the same manner as we averaged the charge density) yield the correct average valence electron energy.

The "cohesive energy" argument of the last paragraph is inaccurate because the repulsive valence-valence terms which enter the cohesive energy should be

---

[18] There is a sudden change in charge density in going across the gap separating L_1 and $L_{2'}$ due to the large mixing of these levels. If L_1 and $L_{2'}$ are averaged and considered as a single double degenerate level, our statement is true.

[19] J. L. Birman, Phys. Rev. 98, 1863 (1955).

TABLE XI. Fourier coefficients of total potential. Column 2 lists the sum of the core Coulomb and core-valence exchange contributions of Table II. Columns 3 and 4 list the sum of the valence Coulomb and valence-valence exchange contributions of Table X for the momentum independent and dependent exchange potentials. Columns 5 and 6 list the sum of column 2 with 3 and 4, respectively. The last three columns list Fourier coefficients of the repulsive potential for $\Gamma_{15}^{(1)}$, $\Gamma_{2'}^{(1)}$, and $\Gamma_1^{(1)}$ states which must be added to the coefficients in columns 5 or 6 to obtain the total effective potential for one of these states. The differences between $V_R(\Gamma_{2'})$ and $V_R(\Gamma_1)$ are due solely to the differences in energy of the two levels.

$\left(\dfrac{a}{2\pi}K\right)^2$	Vcore	$V_{k\text{-indep}}$ val	$V_{k\text{-dep}}$ val	$V_{k\text{-indep}}$ total	$V_{k\text{-dep}}$ total	$V_R(\Gamma_{15})$	$V_R(\Gamma_{2'})$	$V_R(\Gamma_1)$
0	?	?	?	−2.9	−2.695[a] −3.305[b]	0.523	0.801	0.720
3	−0.793	0.078	0.105 0.059	−0.715	−0.688[a] −0.764[b]	0.391	0.618	0.558
8	−0.368	−0.008		−0.376		0.265	0.429	0.390
11	−0.294	−0.003		−0.297		0.221	0.358	0.327
16	−0.229	−0.001		−0.230		0.173	0.276	0.254
27	−0.163	0		−0.163		0.115	0.177	0.166
40	−0.124	0		−0.124		0.079	0.121	0.116
64	−0.086	0		−0.086		0.048	0.078	0.077

[a] For all other states.   [b] For states $L_1^{(1)}$, $L_{2'}^{(1)}$, $\Gamma_1^{(1)}$, $X_1^{(1)}$.

included twice in calculating one-electron energies.[20] This effect can be estimated as follows. According to Slater's rules[9,10] in calculating one-electron energies the valence electrons screen the core by about $0.3e$. The value of V_{000} discussed above may therefore be too negative by an amount $|V_{000}|0.15/0.85\cong0.3$ ry. This quantity is of the order of correlation energies in the solid and it is not certain that such terms can be represented as a one-electron potential. We have therefore neglected this correction in our calculations; it will be seen later that uncertainties in V_{000} of order 0.3 ry have a small effect on the relative positions of the bands.

We used $V_{000}=-2.90$ ry for our k-independent potential and $V_{000}=-3.00$ ry for our k-dependent exchange potential. The correct values can be determined self-consistently to be -3.00 and -3.03 ry; as the differences are small and in the direction of the correction discussed in the preceding paragraph, we did not improve our self consistency. These values of V_{000} are to be compared with the -2.00 ry obtained by Woodruff using the spherical approximation.

In the Appendix of I we discussed various approximations to the valence-valence exchange potential of diamond-type crystals. We concluded that two physically reasonable approximations to this potential yielded satisfactory results for diamond. These were the Slater free-electron approximation [Eq. (3.4)] and a momentum-dependent free-electron approximation. In the case of diamond only the (111) coefficient of the valence-valence exchange potential was large. In Si, because the core is larger the Slater approximation yields significant higher Fourier coefficients for this potential. In this case it is important to include the nonlocal nature of the exchange potential. This can be done by using Brooks' "exchange-correlation hole" formula,

$$V_{\text{Brooks}}{}^K\cong2.97V_{\text{Slater}}{}^K\{[1+0.3(Kr_s)^2]^{-1}$$
$$-\tfrac{2}{3}[1+0.3(Kr_s)^2]^{-2}\},\quad (4.5)$$

[20] F. Seitz, *The Modern Theory of Solids* (McGraw-Hill Book Company, New York, 1940).

which was also discussed in the Appendix of I [Eq. (A.9)]. The effect of this refinement is to leave $V_{111}{}^{\text{val-val ex}}$ practically unchanged but to reduce higher Fourier coefficients quite substantially.

The various approximations just discussed were combined to yield two valence-valence exchange potentials. The first is the momentum-independent potential given by Eq. (4.5). The second is based on the observation that in a free electron gas the exchange potential is momentum dependent with the strength of the potential at the Fermi surface $\tfrac{2}{3}$ and at $k=0$, $\tfrac{4}{3}$ its average value. We probably make a small overestimation of the momentum dependence when we arbitrarily assume that the s part of $L_1^{(1)}$, $L_2^{(1)}$, $X_1^{(1)}$, and $\Gamma_1^{(1)}$ all experience an exchange potential appropriate to $k=0$ and the remaining states listed in Table XII except $\Gamma_{12'}$ experience the potential appropriate to k_F. $\Gamma_{12'}$ which contains no plane waves below (200) in a free electron gas picture experiences an exchange potential only 62% as strong as those states on the Fermi surface. We have used both these potentials to calculate this level. In semiconductors ρ is nearly constant and may be written

$$\rho=(32/a)\{1+\textstyle\sum_K \rho_K e^{i\mathbf{K}\cdot\mathbf{r}}\}. \quad (4.6)$$

where a is the lattice constant $=10.263$. For silicon the calculation of the exchange potential is greatly simplified by making the approximation (which is well justified here)

$$\rho^{\frac{1}{3}}\cong(32/a)^{\frac{1}{3}}\{1+\tfrac{1}{3}\textstyle\sum_K \rho_K e^{i\mathbf{K}\cdot\mathbf{r}}\}. \quad (4.7)$$

In a free electron gas of the density of silicon the average $V_{000}{}^{\text{exch}}=-0.914$ ry. Hence since our average $V_{000}{}^{\text{total}}=-3.00$ ry, we have $V_{000}{}^{\text{total}}=-3.305$ and -2.695 ry at the bottom and top of the Fermi sea, respectively. From Eqs. (4.7) and (3.4) we compute $V_{111}{}^{\text{val-val ex}}=0.700$ ry; hence $V_{111}{}^{\text{val-val ex}}=-0.0933$ and -0.0467 ry at the bottom and top of the Fermi sea. Table X lists the Fourier transforms of both exchange potentials; the momentum dependence of the higher Fourier transforms which are quite small is neglected.

Table X also compares the nonmomentum dependent valence-valence exchange with Woodruff's. It is interesting to note that the two are quite similar; this is because Woodruff's valence charge distribution is quite similar to ours.

It is our feeling that either of our exchange approximations may be in error by as much as 40% causing errors in V_{111} of up to 0.03 ry. These are the largest uncertainties appearing in this calculation. The reader is referred to the Appendix of I where we give a thorough discussion of the uncertainties inherent in all approximations to exchange and correlation.

The Fourier transforms of the various contributions to the total potential are summed in Table XI for both exchange potentials.

V. ENERGY BANDS

The energy levels are computed by diagonalizing the secular determinant [Eq. (2.8)] and adding the correc-

TABLE XII. Energy levels of various irreducible representations for momentum independent exchange potential (column 2) and assuming $X_1^{(1)}$, $L_1^{(1)}$, $L_{2'}^{(1)}$, and $\Gamma_1^{(1)}$ see valence-valence exchange potential appropriate to $k=0$ and remaining levels appropriate to Fermi surface in a free electron gas (column 3).

	k-indep. exch.	k-dep. exch.
Γ_1	-2.316 ry	-2.787 ry
$L_{2'}$	-2.113	-2.588
X_1	-2.011	-2.464
L_1	-1.964	-2.396
X_4	-1.768	-1.523
$L_{3'}$	-1.701	-1.429
$\Gamma_{25'}$	-1.560	-1.297
$X_1^{(2)}$	-1.383	-1.178
Γ_{15}	-1.348	-1.115
L_3	-1.283	-1.066
$L_1^{(2)}$	-1.184	-0.933
$\Gamma_{12'}$	-1.002	-0.782 (-0.512^{a})
$\Gamma_{2'}$	-0.931	-0.659
$\Gamma_1^{(2)}$	-0.869	-0.652

[a] Assuming $\Gamma_{12'}$ sees only 62% of the exchange potential seen by states on the Fermi surface.

tions of Table VI which is equivalent to diagonalizing the OPW secular determinant. The secular determinant of $\Gamma_{25'}$ contained 469 plane waves; the others contained about 65 except for $\Gamma_{12'}$ which we carried out to a 3×3 matrix (89 pw). Table XII lists the estimated converged energy levels for both exchange potentials. As we remarked in I, beyond 65 plane waves the p levels converge quite similarly and the s levels drop less than the p; as $\Gamma_{25'}$ drops only 0.009 ry after 65 pw, the estimated converged levels should be in error by no more than 0.004 ry. In Fig. 3 the convergence of various levels (nonmomentum dependent potential) is shown out to 65 pw.

Orthogonalization to incorrect core functions causes the valence wave functions to converge slowly and with incorrect eigenvalues. In Fig. 4 we compare the convergence of the $\Gamma_{25'}$ level using our nonmomentum dependent potential and using Woodruff's. For the sake of
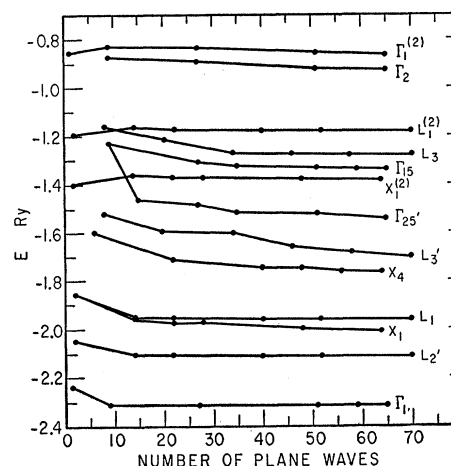
FIG. 3. Convergence of various valence term levels (k-independent potential) as a function of the number of plane waves used in the expansion.

comparison we took $V_{000}=-2.9$ ry and $E-E_n=7.18$ ry for Woodruff's $\Gamma_{25'}$ (hereafter called $\Gamma_{25'}^{W}$) as well as ours. (Using $V_{000}=-2.9$ ry, $E-E_n$ is actually 6.4 ry for $\Gamma_{25'}^{W}$ making his repulsive potential even weaker; on the other hand, using his value of $V_{000}=-2.0$ ry, $E-E_n=7.3$ ry.)

Figure 4 gives an indication of how much of the poor convergence found in other semiconductor calculations throughout the literature may be attributed to the valence bond and how much is due to errors in orthogonalization. Even when the correct core wave functions are used, $\Gamma_{25'}$ drops about 0.3 ry on going from a 1×1 reduced matrix (9 plane waves) to a 6×6 matrix (65 pw); it drops only another 0.009 ry on going to a 34×34 matrix (469 pw). On the other hand, $\Gamma_{25'}^{W}$ drops 0.023 ry on going from a 6×6 to a 34×34 matrix and converges to a level 0.22 ry below $\Gamma_{25'}$. (This absolute difference is meaningful as the same V_{000} was used in both cases.) It should be pointed out that most of this difference is not due to $\Gamma_{25'}^{W}$ collapsing into the core region. $\Gamma_{25'}^{W}$ falls below $\Gamma_{25'}$ because the tail of Woodruff's $2p$ eigenfunction is too small, making the effective potential in the bonding region between atoms too attractive. Had Woodruff's $2p$ tail been too big, $\Gamma_{25'}^{W}$ would have appeared to lie above our $\Gamma_{25'}$. Only after a large number of plane waves (perhaps 100 000) would it collapse into the core region and drop below $\Gamma_{25'}$.
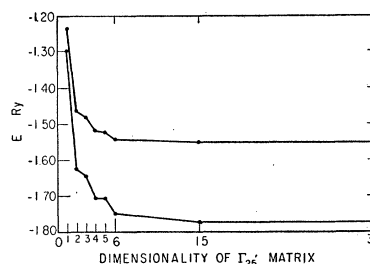
FIG. 4. Comparison of the convergence of $\Gamma_{25'}$ obtained by us (upper curve) and obtained by Woodruff (lower curve) as a function of dimensionality of reduced matrix.
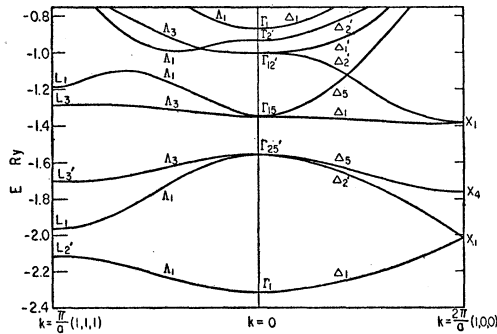
FIG. 5. Sketch of the energy bands of silicon along (100) and (111) axes of the Brillouin zone for the k-independent potential.

The energy bands are sketched for both potentials in Figs. 5 and 6. The shape of the bands was determined from a knowledge of the slopes at points of high symmetry, the location of the conduction band minimum, and the interpolation scheme of one of us.[21] The differences between Figs. 5 and 6 are an indication of the uncertainties in the energy bands due to uncertainties in valence exchange and correlation.

The indirect energy gap, which is about 0.01 ry less than the $\Gamma_{25'} - X_1^{(2)}$ difference, is known experimentally to be 0.09 ry; we obtain a $\Gamma_{25'} - X_1^{(2)}$ difference of 0.18 ry for the momentum independent exchange calculation and 0.12 ry for the momentum dependent exchange calculation. In the case of diamond both exchange potentials gave good agreement with experiment on the energy gap; this is qualitatively the case here also.

We obtain for the momentum independent and dependent exchange calculations of the valence band width values of 10.3 and 20.3 ev, bracketing the value of 16.7 ± 0.1 ev obtained from soft x-ray emission spectra[22] and indicating that our simple approximation to the momentum dependence of the exchange is qualitatively correct but tends to overestimate the effect. This may be due to our neglect of the effects of correlation on the momentum dependence of V_{000} or simply to the nonfree-electron nature of the problem.

Because Γ_{15} is not a point of minimum energy but rather a saddle point, the onset of direct optical transitions in silicon has not been observed.[23] We can, however, make a very good estimate of the direct gap, as the magnitudes of both the direct and indirect gaps are due primarily to the large drop in $\Gamma_{25'}$. We assume the direct and indirect gaps to vary consistently as we go from our momentum independent potential to our momentum dependent potential to the true crystal potential; knowing the experimental value for the indirect gap, we estimate the direct gap to be 0.17 ry. This direct energy gap plays an important role in the determination of the

hole effective masses which are calculated in the next section.

Some of the results of our calculation are rather surprising at first sight; $\Gamma_{2'}$ is about 0.44 ry above Γ_{15} and even lies about 0.1 ry above $\Gamma_{12'}$ (when $\Gamma_{12'}$ is assumed to see the same exchange potential as Γ_{15}). It is known for germanium that $\Gamma_{2'}$ lies below both Γ_{15} and $\Gamma_{12'}$ and with so much similarity between the two crystals a relative change of $\frac{1}{2}$ ry between two energy levels is unexpected. With the aid of the repulsive potential we can see qualitatively how this comes about. Γ_{15} contains a term $-V_{220}$ and $\Gamma_{12'}$ contains $-2V_{220}$ in the (11) matrix element. $\Gamma_{2'}$ contains a term $+3V_{220}$ in the (11) matrix element making the $\Gamma_{2'} - \Gamma_{15}$ and $\Gamma_{2'} - \Gamma_{12'}$ differences very sensitive to V_{220} and raising $\Gamma_{2'}$ here considerably above Γ_{15} [V_{220} is positive here for s states because the s repulsive potential has a larger (2,2,0) Fourier transform than the true crystal potential]. In Fig. 1, we show a plot of the total effective charge $Z(r) = rV(r)$ for $\Gamma_{2'}$. Now

$$V(\mathbf{K}) = \frac{1}{\Omega} \int V(\mathbf{r}) e^{i\mathbf{K} \cdot \mathbf{r}} r^2 \sin\theta \, dr \, d\theta \, d\varphi$$

$$= \frac{4\pi}{\Omega K} \int Z(r) \sin Kr \, dr. \quad (5.1)$$

We note that $\sin Kr$ is much larger in the core for $\mathbf{K} = (2\pi/a)(2,2,0)$ than for $\mathbf{K} = (2\pi/a)(1,1,1)$ and is near its maximum where $Z(r)$ changes sign. In germanium the attractive potential is much stronger in the core region than in silicon; furthermore the repulsive s and p potentials should drop off faster in the outer core region than the shielding of the d electrons builds up. Hence, V_{220}, which is most strongly affected by these changes which occur in the region where $\sin[(2\pi/a)(2,2,0)] = 1$, very likely is sufficiently more negative in germanium for both $\Gamma_{2'}$ and Γ_{15} to cause the required effect.
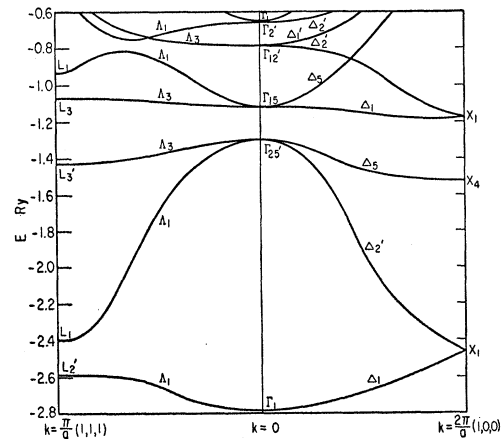

FIG. 6. Sketch of the energy bands of silicon along (100) and (111) axes of the Brillouin zone where the valence-valence exchange potential of the states $L_1^{(1)}$, $L_{2'}^{(1)}$, $\Gamma_1^{(1)}$, and $X_1^{(1)}$ is taken to correspond to that of free electrons at $k=0$ and the remaining states to that of free electrons at the Fermi surface.

[21] J. C. Phillips, Phys. Rev. **112**, 685 (1958).

[22] D. H. Tomboulian and D. E. Bedo, Phys. Rev. **104**, 590 (1956).

[23] W. Paul, J. Phys. Chem. Solids **8**, 196 (1959).

According to Herman's calculation, in diamond $\Gamma_{12'}$ lies above $\Gamma_{2'}$ by about 0.8 ry (about 0.35 ry when scaled to the silicon lattice). This is because the lowest plane wave appearing in the $\Gamma_{12'}$ irreducible representation is a (200) plane wave. This adds (for silicon) to the lowest $\Gamma_{12'}$ solution a kinetic energy 0.375 ry above that of the lowest $\Gamma_{2'}$ solution. However, because silicon has $2s$ and $2p$ core functions, the repulsive potential seen by s and p states is about 0.4 ry stronger than in diamond. $\Gamma_{12'}$ having d symmetry about the atoms does not see this repulsive potential and hence its relative position in silicon is lower than in diamond by the amount of this additional repulsive potential.

Throughout this paper we have estimated errors in the potential wherever they were committed. We shall here estimate the effect of these errors on $\Gamma_{25'}$ and hence on the direct and indirect gaps. Like all p levels, the matrix elements of $\Gamma_{25'}$ contain only differences of Fourier transforms; in particular, the (21) matrix element is $2(V_{111}-V_{311})$. For small changes in the potential the change in this quantity is very nearly equal to the change in $\Gamma_{25'}$. Hence the uncertainties in V_{111} of 0.03 and 0.015 ry due to uncertainties in valence-valence exchange and the self-consistent valence Coulomb potential cause errors of 0.06 and 0.03 ry in $\Gamma_{25'}$. The uncertainty of 0.3 ry in V_{000} causes uncertainties through the repulsive potential in V_{111} and V_{311} of 0.013 and 0.0087 ry, giving an error in $\Gamma_{25'}$ of less than 0.01 ry.

We have neglected several very small contributions to the potential. From Heine's[6] aluminum calculation and Eq. (5.1), we estimate an error in $\Gamma_{25'}$ of about 0.001 ry from our omission of core polarization (valence-core correlation). Spin-orbit coupling is an omission of about[24] 0.003 ry in $\Gamma_{25'}$. The effect of the overlap of the core eigenfunctions on the repulsive potential can be estimated by adding an exponential tail to the core functions. A straightforward computation shows this leads to a change in $\Gamma_{25'}$ of less than 10^{-4} ry.

We conclude this section by remarking that near the energy gap the band structure shown in Figs. 5 and 6 is approximately the same as that discussed by Phillips.[21] Phillips showed that such a structure was in good agreement with all that can, at present, be inferred experimentally about the positions of various levels; he also estimated effective masses, neglecting orthogonalization corrections. All such corrections are included in the calculations of the following section.

VI. EFFECTIVE MASSES OF HOLES AND ELECTRONS

The results of the last section suggest that the wave functions obtained in this paper are sufficiently accurate to justify a detailed calculation of the effective masses of electrons and holes in Si which have been measured by cyclotron resonance; these quantities provide a most severe test of the correctness of the calculation. For this

[24] R. J. Elliott, Phys. Rev. **96**, 266 (1954).

TABLE XIII. Symmetry about point midway between atoms and atomic character of basis functions of irreducible representations appearing in effective mass parameters of holes at the top of the valence band.

I. R.	Basis	Sym.	Atomic character
$\Gamma_{25'}$	ϵ_1'	yz	bonding $p_x{}^{(3)}$
$\Gamma_{2'}$	β'	xyz	antibonding $s^{(1)}$
$\Gamma_{12'}$	γ_1'	$(x^2+wy^2+w^2z^2)^aI^b$	antibonding $d_{x^2+wy^2+w^2z^2}{}^{(2)}$
Γ_{15}	δ_3	z	antibonding $p_z{}^{(3)}$
Γ_{25}	ϵ_3	xyI^b	antibonding $d_{xy}{}^{(3)}$

a $w^3=1$.
b Odd under inversion.

purpose it is again convenient to divide the crystal functions into their smooth and oscillatory parts:

$$\psi_\alpha = C_\alpha(\varphi_\alpha + \textstyle\sum_r a_n{}^\alpha \psi_\alpha{}^n), \quad (\varphi_\alpha, \varphi_\alpha)=1, \quad (6.1)$$

where C_α is chosen to normalize ψ_α. This division is convenient because the interband matrix elements of $\mathbf{p}$ which determine the effective masses are derived largely from the φ_α terms, the oscillatory terms making only a small contribution. Because φ_α has been expanded in plane waves, matrix elements of $\mathbf{p}$ for it are easily calculated; the oscillatory terms, being small, are then treated using analytic approximations.

We consider first the holes at $\Gamma_{25'}$. It is well known that under the spin-orbit perturbation the $\Gamma_{25'}$ level at the top of the valence band splits into two levels. By second-order degenerate perturbation theory the $p_{\frac{3}{2}}$ level which lies about 0.003 ry above the $p_{\frac{1}{2}}$ level can be shown to split into two doubly degenerate levels as one moves away from the center of the Brillouin zone.[25,26]

$$E(k) = Ak^2 \pm [B^2k^4 + C^2(k_x{}^2k_y{}^2 + k_y{}^2k_z{}^2 + k_z{}^2k_x{}^2)]^{\frac{1}{2}}, \quad (6.2)$$

where, according to Dresselhaus,[25]

$$A = \tfrac{1}{3}(F+2G+2H_1+2H_2)+1, \quad (6.3a)$$

$$B = \tfrac{1}{3}(F+2G-H_1-H_2), \quad (6.3b)$$

$$C^2 = \tfrac{1}{3}[(F-G+H_1-H_2)^2 - (F+2G-H_1-H_2)^2], \quad (6.3c)$$

in units of $\hbar^2/2m$, and where

$$H_1 = 4\sum_{\Gamma_{15}} \frac{|\langle \epsilon_1'|d/dy|\delta_{3l}\rangle|^2}{E_0 - E_l}, \quad (6.4a)$$

$$H_2 = 4\sum_{\Gamma_{25}} \frac{|\langle \epsilon_1'|d/dy|\epsilon_{3l}\rangle|^2}{E_0 - E_l}, \quad (6.4b)$$

$$F = 4\sum_{\Gamma_{2'}} \frac{|\langle \epsilon_1'|d/dx|\beta_l'\rangle|^2}{E_0 - E_l}, \quad (6.4c)$$

$$G = 4\sum_{\Gamma_{12'}} \frac{|\langle \epsilon_1'|d/dx|\gamma_{1l}'\rangle|^2}{E_0 - E_l}, \quad (6.4d)$$

[25] G. Dresselhaus, A. F. Kip, and C. Kittel, Phys. Rev. **98**, 368 (1955).
[26] G. Dresselhaus, Ph.D. thesis, University of California, 1955 (unpublished).

TABLE XIV. The energy denominator of the first term, the first term of the sum and the total H_1, H_2, F and G (neglecting orthogonalization effects) together with the effective mass parameters A, B, and C calculated therefrom. The experimental values of H_1, F, and G are computed from the experimental values of A, B, and C assuming $H_2=0$.

	E_0-E_1	First term	Sum	Experiment
H_1	0.170	−6.19	−6.21	−6.1
H_2	2.10	−0.01	−0.01	∼0
F	0.638	−1.65	−2.14	−2.1
G	0.785	−0.78	−0.78	−0.35
A			−4.38	−4.0±0.1
B			0.84	1.1±0.4
C			±4.11	±4.1±0.4

with E measured in ry. Table XIII lists the basis functions appearing in Eqs. (6.3) together with their symmetry and their atomic character.

The calculation of the four matrix sums of Eqs. (6.4) is straightforward and simple when only φ_α is retained in (6.1). The second column of Table XIV lists the value of E_0-E_1 used in computing the four sums. With the exception of $E(\Gamma_{15})-E(\Gamma_{25'})$ which was discussed at the end of Sec. V, they are all taken directly from the momentum dependent valence-valence exchange calculation as are the basis functions. Column 3 lists the first term in the sum and column 4 lists the four matrix sums as computed from the smooth part of the wave functions (i.e., the basis functions composed only of plane waves).

The three parameters A, B, and C may be experimentally determined by fitting the cyclotron resonance hole effective mass curves (see reference 26). The most accurate values are probably those given by Lax[27]: $A=-4.0\pm0.1$, $|B|=1.1\pm0.4$, $|C|=4.1\pm0.4$. Taking $H_2=0$ and neglecting the experimental uncertainties, Eqs. (6.3) may be solved for F, G, and H_1. There are two sets of solutions; the physically reasonable set is listed in column 5 of Table XIV. Agreement of theory with experiment is seen to be excellent for F, H_1, and H_2 but the theoretical value of G is seen to be too large by a factor of two. Because of the experimental uncertainties and the small value of G, little significance should be attached to this point.

An exact but extremely cumbersome calculation of the effective masses can be made using orthogonalized plane waves. We here approximate the effect on the effective masses of the oscillations in the wave functions in the core region using the spherical approximation for the core region. Because the resulting corrections turn out to be small we may approximate the core orbitals by Woodruff's analytic functions.[7] The valence wave functions in the core region then have the form,

$$\psi_{3s}=0.2568(e^{-0.566r}-26.79re^{-4.925r}$$
$$+6.625e^{-13.7r}), \quad (6.5a)$$

$$\psi_{3p}(z)=0.7995z(e^{-1.13r}-11.39e^{-4.925r}), \quad (6.5b)$$

[27] B. Lax, Rev. Modern Phys. 30, 122 (1958).

$$\psi_{3d}(xy)=1.262xye^{-r}, \quad (6.5c)$$

$$\psi_{3d}(x^2+wy^2+w^2z^2)=0.515(x^2+wy^2+w^2z^2)e^{-r},$$
$$(w^3=1). \quad (6.5d)$$

ψ_{3s} and ψ_{3p} follow from Eqs. (3.6); the choice of the factor 1 in the exponential of the d functions is somewhat arbitrary but the results do not depend strongly on it. The normalization C_{3s} of $\psi_{3s}=1.069$ and $C_{3p}=1.044$.

The leading terms in Eqs. (6.5) represent analytic approximations to φ_α in the core region. They are the only terms which are large outside the core. Matrix elements of p involving φ_α alone can be taken from the results quoted above which were obtained using the plane-wave expansion of φ_α which is valid throughout the unit cell. Terms involving core orbitals will be large only in the core region, where Eqs. (6.5) represent an adequate approximation. In this way we find two corrections to the values previously obtained above using φ_α only. The first of these, which is the larger here, stems solely from the changed values of C_α; this correction is listed in column 3 of Table XV. The second and more obvious correction comes from the cross terms involving core orbitals; this is shown in column 4. The contribution of the core to H_1 can be seen to be zero by symmetry.

The values of H_1, H_2, F, and G including core effects are given in the last column of Table XV. The results, while only approximate, give a fairly good indication of the effect of the oscillations of the wave functions in the core region on the effective masses. The inclusion of these effects slightly worsens agreement with experiment; the values of A, B, and C are still correct to about 30%.

It has been suggested by Kane[28] and Phillips[29] that the non-local nature of exchange and correlation potential tends to make the experimental values of F, G,

TABLE XV. Column 2 lists the values of H_1, H_2, F and G computed from the smooth part of the wave function. When it is orthogonalized to the core the smooth part must be renormalized leading to the changes listed in column 3. Column 4 lists the direct contribution from the orthogonalization terms and column 5 lists the sum of columns 2, 3, and 4 together with the recalculated effective mass parameters A, B, and C.

	Smooth	Renorm.	Core	Total
H_1	−6.21	−1.17	0	−7.37
H_2	0.01	−0.001	0	−0.01
F	−2.14	−0.52	0.58	−2.08
G	−0.78	−0.07	0.004	−0.85
A				−5.18
B				1.20
C				±4.12

[28] E. D. Kane, J. Phys. Chem. Solids 6, 236 (1958).
[29] J. C. Phillips, J. Phys. Chem. Solids 7, 52 (1958). The discrepancy between the matrix elements of reference 29 and this paper stems mainly from the values of a_0 and b_0 assumed there. While these are appropriate to Woodruff's Si calculation, a_0 and b_0 there are too small because V_{111}^{eff} is too attractive. The normalization correction included here also contributes a significant change to the results of reference 29.

and H larger than the calculated one-electron values. The sign of this correction, though not its magnitude, is uniquely determined by "exchange and correlation hole" arguments. While physically plausible these semi-classical arguments may fail in semiconductors, as was pointed out in the Appendix to I. We are inclined to believe that such is the case here, for if corrections as large as those suggested by reference 29 are used (and these are only half as large as predicted by the Slater model of reference 28) the calculated values will differ from the experimental ones by a factor of 2.

We now turn to the case of the electrons at Δ. The minima of the conduction band occur at the six equivalent points $(2\pi/a)(\alpha,0,0)$ where from both experimental and theoretical data[21] $\alpha \approx 0.86$. The energy as a function of distance from the k_x minimum is given in ry by[26]

$$E = E_0 + K_x{}^2(1+G_1) + (K_y{}^2 + K_z{}^2)(1+G_2), \quad (6.6)$$

where

$$G_1 = 4 \sum_{l \neq 2} \frac{|\Delta_1{}^{(2)}| d/dx |\Delta_1{}^{(l)}|}{E_0 - E_l}, \quad (6.7a)$$

$$G_2 = 4 \sum_{l} \frac{|\Delta_1{}^{(2)}| d/dy |\Delta_{51}{}^{(l)}|}{E_0 - E_l}, \quad (6.7b)$$

where $\Delta_{51}{}^{(l)}$ is the eigenfunction transforming like y of the lth twofold degenerate Δ_5 level and $\Delta_1{}^{(l)}$ is the eigenfunction of the lth Δ_1 level. Hence we may write

$$E = E_0 + (m_L{}^*/m)K_x{}^2 + (m_T{}^*/m)(K_y{}^2 + K_z{}^2), \quad (6.8)$$

where

$$m_L{}^*/m = (1+G_1)^{-1}; \quad m_T{}^*/m = (1+G_2)^{-1}. \quad (6.9a, b)$$

G_1 and G_2 were calculated in the same manner as the matrix sums H_1, H_2, F, and G and yield $m_L{}^*/m = 0.971$, $m_T{}^*/m = 0.205$.[30] The experimental values of reference 25 are $m_L{}^*/m = 0.97$, $m_T{}^*/m = 0.19$.

Thus again in the case of electron effective masses we find good agreement with experiment. Such agreement would not have been found had we used wave functions

derived from Woodruff's incorrect repulsive potential (which was too weak). For his potential not only is the energy gap too large but the leading coefficient a, in the expansion of $\varphi_\alpha = \sum_i a_i \langle K_i \rangle$ (where $\alpha = \Gamma_{25'}$ or Δ_5) is too small; the corresponding values of the various constants, especially H_1 and G_2 are too small. (The same comment probably applies to the calculations of Herman[31] for Ge.) From the results that we have presented it appears that we can again conclude that our calculation is correct to within the limits of accuracy imposed by necessary approximations for valence-valence exchange and many-electron interactions.

VII. CONCLUSIONS

There are several conclusions concerning the valence semiconductors to be drawn from this paper and from I. The most important of these is that it is possible in a fairly simple way to obtain semi-quantitative results for the band structure of diamond-type semiconductors. The crystal charge density surprisingly is close to a superposition of free-atom charge densities. The crystal Coulomb potential is therefore easily obtained and the momentum-dependent free-electron approximation can be used to obtain satisfactory values for valence-valence exchange. The only technical point that requires careful treatment is the calculation of the core-orbitals part of the valence wave functions.

The results of a careful calculation can also be used to compute the effective masses in a one-electron, local potential approximation. Comparison of the computed and observed values indicates that these approximations yield good results for at least s and p electrons. Corrections due to the nonlocal nature of the many-particle potential appear to be quite small in this case, and much smaller than had previously been estimated from free-electron arguments.

---

[30] The wave functions at Δ were obtained by extrapolating the wave functions at X. This leads to an uncertainty of less than 0.01 in the values of $m_L{}^*/m$ and $m_T{}^*/m$.

[31] F. Herman, Physica 20, 801 (1954).